

Simulation of diffusionlimited stepgrowth polymerization in 2D: Effect of shear flow and chain rigidity

U. S. Agarwal and D. V. Khakhar

Citation: *The Journal of Chemical Physics* **99**, 3067 (1993); doi: 10.1063/1.466195

View online: <http://dx.doi.org/10.1063/1.466195>

View Table of Contents: <http://scitation.aip.org/content/aip/journal/jcp/99/4?ver=pdfcov>

Published by the [AIP Publishing](#)

Articles you may be interested in

[Flow enhanced diffusion-limited polymerization of rodlike molecules](#)

J. Chem. Phys. **114**, 553 (2001); 10.1063/1.1330211

[Brownian dynamics simulation of diffusion-limited polymerization of rodlike molecules: Anisotropic translation diffusion](#)

J. Chem. Phys. **108**, 5626 (1998); 10.1063/1.475951

[Brownian dynamics simulation of diffusion-limited polymerization of rodlike molecules: Isotropic translational diffusion](#)

J. Chem. Phys. **107**, 3289 (1997); 10.1063/1.474679

[Diffusionlimited polymerization of rigid rodlike molecules: Semidilute solutions](#)

J. Chem. Phys. **99**, 1382 (1993); 10.1063/1.465382

[Diffusionlimited polymerization of rigid rodlike molecules: Dilute solutions](#)

J. Chem. Phys. **96**, 7125 (1992); 10.1063/1.462546



Simulation of diffusion-limited step-growth polymerization in 2D: Effect of shear flow and chain rigidity

U. S. Agarwal^{a)} and D. V. Khakhar^{b)}

Department of Chemical Engineering, Indian Institute of Technology-Bombay, Powai, Bombay 400076, India

(Received 20 January 1993; accepted 27 April 1993)

Multimolecule Brownian dynamics simulation results for diffusion controlled polymerization of bead-rod chain molecules in 2D solution are presented. Reaction between any two molecules undergoing Brownian diffusion takes place if the reactive chain ends approach each other to within a certain reaction radius, and if the chain end carrying segments are collinear within certain specified limits. The second order reaction rate constant is found to decrease with time as the molecular lengths increase and the diffusivities decrease. Application of a shear flow is seen to result in alignment of the molecules along the flow direction, thereby enhancing the concentration of molecular pairs with parallel orientation of reactive-end carrying chain segments, and hence the overall reaction rate. This effect is found to be more pronounced in the case of long rigid molecules as compared to flexible molecules because of the slow rotation and high level of orientation under flow of the former. Even the molecular weight distribution (MWD) obtained during polymerization may be affected. For example, longer molecules have lower diffusivities and hence lower reactivities, resulting in a narrower MWD in the absence of flow, as compared to the results with the usual assumption of molecular reactivity being independent of chain length. Furthermore, in the presence of an external flow, the longer molecules orient to a higher degree and hence display a higher enhancement in reactivity. This results in a wider MWD of the polymer. The simulation results are in qualitative agreement with previous experimental data for solution polymerization of rod-like molecules.

I. INTRODUCTION

Polymer reactions may become diffusion controlled during bulk or solution polymerization as the molecular weight increases and the diffusivity of the polymer molecules decreases. An important example is the *Tromsdorf effect* in which diffusional limitations slow down the termination reactions in free radical polymerization, resulting in a rapid increase in the molecular weight.¹ Other examples are the propagation step in free radical polymerization, cross-linking polymerization with trapping of chain ends, etc.¹⁻⁴ Instances of diffusion controlled step-growth polymerization have been reported only for rod-like polymers.^{5,6} In this case, the molecules require near-parallel alignment for reaction, and the slow rotational diffusion of the molecules is found to limit the rate of reaction.^{5,6} The analysis of diffusion controlled polymerization has been carried out in several previous works. In case of flexible molecules, segmental diffusion of the chain end is generally the rate controlling step and must be included in the theoretical development.^{1,2,7-9} Recent theoretical analysis of diffusion controlled polymerization of rod-like polymers^{10,11} show that both rotational and translational diffusion of the molecules contribute to the overall rate of reaction, and the mechanisms of the reaction are considerably different as compared to flexible molecules.

An externally imposed shear flow can have two possi-

ble effects on the polymerization reaction (i) an increased number of collisions between molecules due to the local velocity gradient;¹² and (ii) an alignment of polymer chains along the streamlines. Using a simple analysis, it can be shown that (i) would have a negligible effect on the reaction rate due to the small reaction radius.¹² Mechanism (ii), however, could increase the success rate of collisions and thus the reaction rate when reorientation of the colliding segments to a suitable relative configuration is the rate limiting step. Only a few previous studies have considered the effect of flow on polymerization. De Gennes¹³ has stated that the effective reaction rate constant for instantaneous reactions between polymer molecules in a melt is given by

$$k(\dot{\gamma}) = k(0)(\dot{\gamma}\tau_R)^{1/4}, \quad (1)$$

where $\dot{\gamma}$ is the shear rate, τ_R is the terminal relaxation time, and $k(0)$ is the reaction rate constant in the absence of flow. However, details are not given. Silberberg¹⁴ suggested that the reaction rate for polymers can be enhanced by an imposed flow because of the molecular alignment favoring the formation of co-operatively strengthened bonds. In a recent experimental study,⁶ we have shown that the polymerization rate of rod-like molecules is enhanced on application of a shear flow due to orientation of the molecules.

Chain flexibility/rigidity and flow thus play an important role in the course of diffusion controlled polymerizations. An understanding of the role of these effects is important from a practical viewpoint since the rate of polymerization, the molecular weight, and the molecular weight distribution (MWD) are affected by them.⁶ In this

^{a)}Current address: Chemical Engineering Division, National Chemical Laboratory, Pune 411008, India.

^{b)}Author to whom all correspondence should be addressed.

paper, we examine the effects of flow and chain flexibility on step-growth polymerization of bead-rod molecules in solution. Two oligomers are assumed to react instantaneously if the relative orientation and proximity of the chain ends satisfies certain prescribed limits. Due to the complexity of the problem, a multiparticle Brownian dynamics simulation is carried out. Brownian dynamics simulations have been used previously to study the cyclization of single flexible polymer chain.¹⁵ Allison *et al.*¹⁶ have carried out Brownian dynamics simulation of reactions between protein molecules which are required to satisfy certain orientational criteria for reaction. In their approach, the Brownian trajectories for a single molecule in the neighborhood of a reactive sink are used to obtain the overall rate constant. Balazs *et al.*¹⁷ have carried out a 2D simulation of the diffusion controlled clustering behavior of associating flexible polymer molecules containing stickers at each chain end. The main emphasis of the work is the study of the complex branched structures formed. No other previous works have considered a multiparticle Brownian dynamics approach for polymerization.

We first describe the bead-rod chain model for polymer molecules (Sec. II). The simulation procedure and the computational parameters are briefly described in Sec. III. The results are presented in Sec. IV and the conclusions in Sec. V.

II. MODEL DEVELOPMENT

The polymer molecules are modeled as bead-rod chains with mass and hydrodynamic forces concentrated at the beads.¹⁸ The $(m+1)$ beads are linked by m rods, each of which can be considered to represent a chain segment made up of several repeat units. In dilute solution, the chains are assumed to experience negligible interchain forces, and are in relative motion as a combined effect of Brownian diffusion and hydrodynamic forces due to an imposed shear flow. In addition, the motion of the beads and the chain conformation is affected by constraints that maintain the segment length at the equilibrium value L , and the angle α_j between neighboring segments near its equilibrium value α_{eq} . Two chains are assumed to react if the end beads of different molecules approach each other to within the capture radius a , and the relative angle between the end links is close to α_{eq} .

A. Motion of model chains

When inertial forces are neglected, the motion of the i th bead in a $m+1$ bead chain is given by the Langevin equation¹⁹⁻²¹

$$0 = -\zeta \left[\frac{d\mathbf{r}_i}{dt} - \mathbf{v}(\mathbf{r}_i) \right] + \mathbf{A}_i + \mathbf{H}_i + (\mathbf{F}_i - \mathbf{F}_{i-1}), \quad (2)$$

where \mathbf{r}_i is the position vector of the bead i , \mathbf{v} is the imposed bulk velocity, ζ is the Stokes' friction factor, and \mathbf{A}_i is the randomly fluctuating Brownian force acting on the bead. \mathbf{F}_i is the force exerted by the i th and the $(i+1)$ th

beads on each other through the i th link. \mathbf{H}_i is the force on the i th bead due to the angular constraints for the angles between the links α_{i-1} , α_i , and α_{i+1} .

The imposed velocity field in the square domain is taken to be simple shear flow of the form

$$v_x = \dot{\gamma}y. \quad (3)$$

Since in this work we are mainly interested in the enhancement in reaction rate due to orientation by flow, we isolate this from the effect of shear flow on collision rate enhancement. This is achieved by modifying Eq. (3) as

$$v_x = \dot{\gamma}(y - y_{c.m.}), \quad (4)$$

where the subscript c.m. represents the center of mass of the whole molecule.

The bond angle constraint is expressed¹⁹ in terms of a harmonic potential V as

$$\mathbf{H}_i = -\frac{\partial V}{\partial \mathbf{r}_i} \quad (5)$$

with

$$V = \sum_{j=2}^N \frac{1}{2} \gamma_\alpha (\cos \alpha_j - \cos \alpha_{eq})^2, \quad (6)$$

where γ_α is a constant determining the chain rigidity.

The equation for bead displacement in dimensionless form is given by

$$\Delta \xi_i = \mathbf{v}'(\xi_i) \Delta \tau + (\mathbf{F}'_i - \mathbf{F}'_{i-1}) \Delta \tau + \mathbf{B}'_i + \mathbf{H}'_i \Delta \tau, \quad (7)$$

where $\xi_i = \mathbf{r}_i/L$, $\mathbf{v}' = \mathbf{v}L/D$, $\tau = Dt/L^2$, $\dot{\gamma}' = \dot{\gamma}L^2/D$, and all forces are made dimensionless with respect to $\zeta D/L$, with $D = k_B T/\zeta$, k_B being the Boltzmann constant and T being the solution temperature. Also, following Chandrasekhar,²² we have written

$$\mathbf{B}'_i = \int_{\tau}^{\tau+\Delta\tau} \mathbf{A}'_i(\tau) d\tau \quad (8)$$

which has a Gaussian distribution

$$w[\mathbf{B}'_i(\Delta\tau)] = \frac{1}{4\pi\Delta\tau} \exp \left[-\frac{|\mathbf{B}'_i(\Delta\tau)|^2}{4\Delta\tau} \right]. \quad (9)$$

\mathbf{F}'_i are found by simultaneous solution of the m link length constraint equations. Defining

$$\mathbf{q}_i = \xi_{i+1} - \xi_i, \quad (10)$$

the forces \mathbf{F}'_i can be evaluated explicitly at the beginning of a time step by using the identity

$$\mathbf{q}_i \cdot \mathbf{q}_i = 1, \quad \text{for } i = 1, 2, \dots, m, \quad (11)$$

or

$$\mathbf{q}_i \cdot \frac{d\mathbf{q}_i}{d\tau} = 0, \quad (12)$$

which is approximated as

$$[\xi_{i+1}(\tau) - \xi_i(\tau)] \cdot [\Delta \xi_{i+1}(\tau, \Delta\tau) - \Delta \xi_i(\tau, \Delta\tau)] = 0 \quad (13)$$

neglecting changes in q_i over the small interval $\Delta\tau$. To prevent the accumulation of small length changes due to the time discretization errors, each displacement step is followed by a correction step in which bond lengths are adjusted consistently according to the procedure of Ryckaert *et al.*²³

B. Reaction between chains

Two chains of m and n link rods react if the chain ends approach each other within the capture radius (a) and if their relative orientation satisfies the criterion

$$(\cos \alpha_a - \cos \alpha_{eq})^2 < E_{or}, \quad (14)$$

where α_a is the angle of approach between the approaching end segments of the two chains, and E_{or} is a specified parameter and can be considered to be related to activation energy for reaction. If the reaction criteria are satisfied, then the reacting beads of the two chains are merged, and a single chain of $(m+n)$ links is formed.

III. COMPUTATIONS

A random configuration of a number of chains is first generated. By calculating the chain motion in discrete time steps, the molecules are allowed to attain equilibrium configuration under the imposed flow, the Brownian motion, and the intrachain constraints. This is to account for the small time for reorientation under flow as compared to the time of reaction in real systems. In subsequent time, the moving chain molecules are allowed to react and form longer chains if pairs of them satisfy the reaction criteria. The details of the simulation algorithm are as follows:

N_o molecules of m_o links each are initially distributed randomly over the square domain of side L_s . For each molecule, the first bead is placed randomly, and the subsequent bead positions are decided by the equilibrium link length and interlink angle (α_{eq}). The simulation is started at $\tau=0$ and carried out by calculating the bead displacements in discrete steps of time intervals $\Delta\tau$ by numerical integration of the equations of motion for each chain. The molecular positions at the end of each time step are thus determined. Furthermore, at the end of each time step, we calculate the two-dimensional Herman's orientation function defined by

$$\psi(\tau) = (2\langle \cos^2 \theta \rangle - 1), \quad (15)$$

where θ is the angle made by each segment with the x axis. The brackets $\langle \cdots \rangle$ denote an average over all the segments of all the molecules at a time. This procedure is followed until the steady state is attained under the imposed flow, indicated by the flattening of the ψ - τ curve. Thus, the equilibrium conformation of the chains is obtained before the reaction is triggered. At this time, all molecular pairs are examined to find if they satisfy the reaction criteria. Those satisfying the reaction criteria are repeatedly translated randomly over the square domain, so that none of the molecular pairs satisfy the reaction criteria any more. The clock is set again to $\tau=0$, the simulation is restarted, and carried out in discrete time steps, but with the additional

TABLE I. Dimensionless parameters for Brownian dynamics simulation.

$N_o=100$	$\alpha_{eq}=\pi$ rad
$a'=0.2$	$E_{or}=2.5 \times 10^{-7}$
$\dot{\gamma}'=0-100$	$\gamma'_a=0, 1000$
$\Delta\tau=0.0002$	$L_s=10$

consideration that all molecular pairs are examined at the end of each time step to find if they satisfy the reaction criteria. The two molecules of any such pair are translated towards each other along the shortest path (smaller than a) to join at the reactive beads and to form a single longer molecule. At the end of each time step, we calculate the following parameters: The number and weight average degrees of polymerization are obtained from

$$\bar{m}_n = \sum_i iN(i) / \sum_i N(i) \quad (16)$$

and

$$\bar{m}_w = \sum_i i^2 N(i) / \sum_i iN(i), \quad (17)$$

respectively, where $N(i)$ is the number of molecules with i initial repeat units (each of m_o links). The polydispersity index is

$$p = \bar{m}_w / \bar{m}_n \quad (18)$$

and the distribution of weight fraction of chain lengths is calculated from

$$n_w(i) = iN(i) / \sum_i iN(i). \quad (19)$$

In addition, the root mean square (rms) displacement of the beads ($\Delta \xi_{\text{bead}}^{\text{rms}}$) and the chain center of mass ($\Delta \xi_{\text{c.m.}}^{\text{rms}}$), and the root mean square rotation of the end-to-end connector ($\Delta \theta_{\text{e-e}}^{\text{rms}}$), during each time step $\Delta\tau$, are calculated by averaging over all the chains. When plotted against time (τ) or \bar{m}_n , these serve as indicators of the molecular length dependence of the corresponding diffusivities at small times $o(\Delta\tau)$.

The dimensionless parameters used in the simulations are listed in Table I. The equilibrium configuration angle (α_{eq}) is taken so that adjacent links in a chain are collinear. A relatively large reaction radius (a') is taken to ensure a high rate of reaction, and a small value of E_{or} is used to impose a severe relative orientation requirement for reaction ($|\alpha_a - \alpha_{eq}| \leq 0.01$ rad for reaction). The effect of flow is evaluated by considering three different shear rates ($\dot{\gamma}'=10, 20$, and 100) besides the no flow case ($\dot{\gamma}'=0$). In addition, the starting molecules are taken to be either single link ($m_o=1$) or four links each ($m_o=4$), and two different values for the chain rigidity (γ'_a) are used (Table I). $\gamma'_a=0$ corresponds to flexible chains and a high value of γ'_a corresponds to rigid chains. Model *A* corresponds to initially short, rigid chains ($m_o=1, \gamma'_a=1000$). Model *B* corresponds to long ($m_o=4$) stiff ($\gamma'_a=1000$) molecules and model *C* corresponds to long ($m_o=4$) flexible ($\gamma'_a=0$) molecules. Comparison of the results of model *A* with

model *B* would show the effect of chain length and the comparison of the results of model *C* with model *B* should reflect the effects of chain flexibility.

The time step ($\Delta\tau$) and system size (L_s) are computational parameters. The time step is taken to be small enough ($\Delta\tau=0.0002$) so that no otherwise feasible reaction encounter would be missed and system size ($L_s=10$) is taken to be large enough that the results are not affected by further increase in L_s . The time step is also taken to be small enough relative to the stiffness parameter (γ'_a) so that unrealistic displacements due to the bond angle constraints are avoided. The use of a predictor-corrector method for the integration step further precludes such effects. Each run is carried to desired time (τ) of reaction. The \bar{m}_n , p , $n_w(i)$, and the rms displacement and rotation results are smoothed by averaging for 100 different initial configurations of the molecules. Each case required nearly 10^5 central processing unit (CPU) seconds of computing time on Cyber 180/840.

IV. RESULTS AND DISCUSSION

A. Orientation development

In the absence of flow, the orientation function (ψ) is nearly zero in all cases, corresponding to random orientation in 2D space. The primary consequence of the shear flow is to reorient the molecules along streamlines. The evolution of the orientation function is plotted in Fig. 1. (The error bars in the figures denote the maximum and minimum values obtained for three different runs.) In each case, the orientation initially increases and then reaches a steady state. For the case *A* ($m_o=1$), we note that at higher shear rates, the initial rise in orientation factor is faster and a higher level of steady state orientation is obtained [Fig. 1(a)]. Comparing between different models for the same shear rate ($\dot{\gamma}'=10$), we find that a higher level of steady state orientation is obtained for the longer and more rigid chains (model *B*) [Fig. 1(b)].

B. The effect of diffusional limitations on reaction

Based on Flory's²⁴ assumption of molecular reactivity being independent of chain length, for a second order step-growth homogeneous solution polymerization, the number average degree of polymerization is expected to rise linearly with time

$$\bar{m}_n = (M_o)k'\tau + 1, \quad (20)$$

where (M_o) is the initial monomer concentration and k' is the rate constant. Thus the slope of the \bar{m}_n - τ curve is proportional to the overall reaction rate constant (k'), and a reduction in the slope would indicate a reduction in the reaction rate constant. For our simulations, the evolution of \bar{m}_n in the absence of flow is presented in Fig. 2. The slope of the \bar{m}_n - τ curve decreases initially ($\tau < 0.1$), corresponding to the transient effects which occur, while the local concentration gradients about each sink achieve their steady values.²⁵ At later times, the curves obtained are nearly linear, corresponding to a nearly steady state rate constant. Such a steady state is generally not possible for

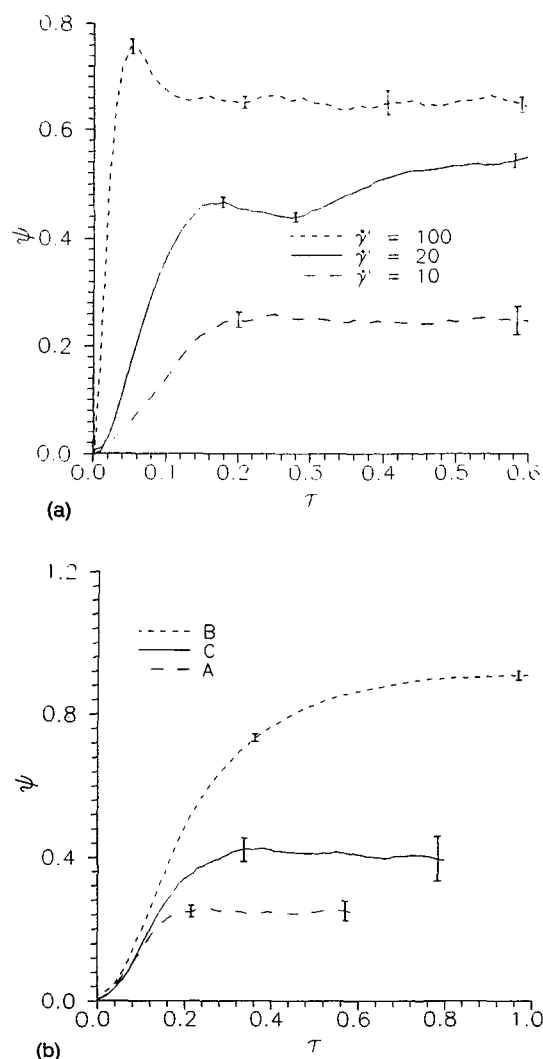


FIG. 1. (a) Increase in the orientation function (ψ) with time (τ) for model *A* at different shear rates. (b) Increase in the orientation function (ψ) with time (τ) for the three different models at $\dot{\gamma}'=10.0$.

diffusion and reaction in 2D systems in which the rate constant is found to decrease with time.²⁶ However, in this case, a steady state is reached because of the additional dimension for diffusional flux contributed by the configurational diffusion of the reactive segments with respect to the molecular coil center. At still longer times ($\tau > 0.8$), the reducing slope for model *A* is an indication of the increasing severity of the diffusional limitations with increase in \bar{m}_n . An examination of the rms displacements per step for each bead ($\Delta\xi_{\text{bead}}^{\text{rms}}$) and for the center of mass of each molecule ($\Delta\xi_{\text{c.m.}}^{\text{rms}}$), and the rms rotation of the end-to-end vector ($\Delta\theta_{\text{e-e}}^{\text{rms}}$) shows that the translational and rotational diffusivities of molecules *A* indeed decrease with progress of reaction (Figs. 3–5). However, for models *B* and *C*, the reduction in the rms displacements in the range of \bar{m}_n considered is smaller (Figs. 3–5), and correspondingly, the slope of the \bar{m}_n - τ curves is nearly constant (Fig. 2). The slope of the \bar{m}_n - τ curves (Fig. 2), and hence the rate constant, is also lower for the longer chains (models *B* and *C*, compared to model *A*) because of their lower dif-

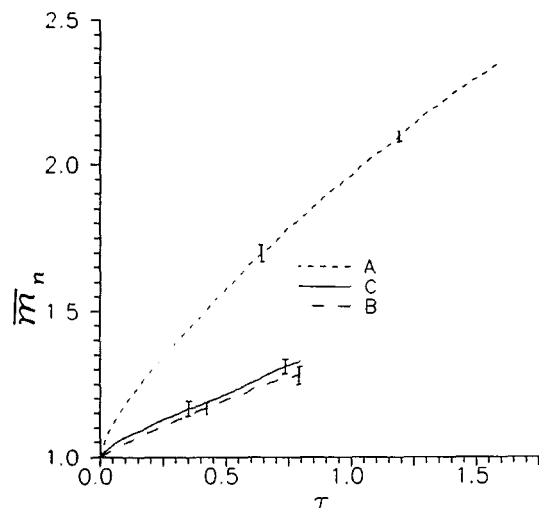


FIG. 2. Increase in size (\bar{m}_n) of the chain molecules with time of reaction (τ) for the three different models in the absence of flow.

fusivities (Figs. 3–5). The progress of reaction in the absence of flow is comparable for the flexible chains (model C) and the rigid chains (model B) (Fig. 2), and this is because their diffusivities are nearly the same (Figs. 4 and 5).

Since the polydisperse polymerization system is made of chains of different lengths, an additional implication of the lower diffusivity of longer chains is the lower reaction rate constant for the longer molecules. While Flory's assumption of molecular reactivity being independent of chain lengths predicts that the polydispersity (p) increases linearly with conversion ($x = 1 - 1/\bar{m}_n$)

$$p = 1 + x, \quad (21)$$

we find (Fig. 6) that p for model A is smaller than this prediction for high conversion ($x > 0.25$). This is because

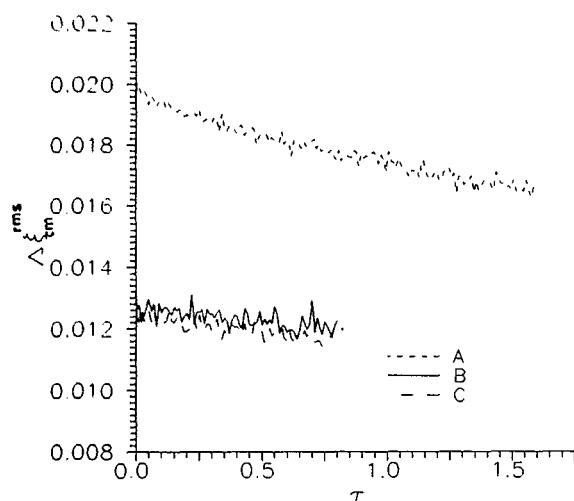


FIG. 3. Variation of root mean square displacement per time step of the chain center of mass (Δz_{cm}^{rms}) for the three different models with reaction time (τ) in the absence of shear flow.

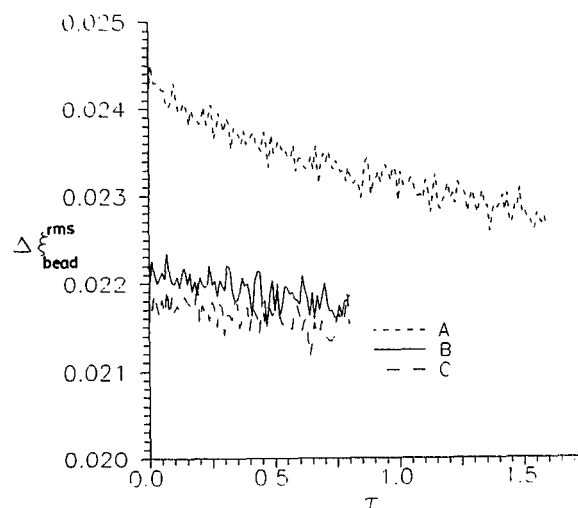


FIG. 4. Variation of the root mean square displacement per time step of each bead (Δz_{bead}^{rms}) for the three different models with reaction time (τ) in the absence of shear flow.

of the reduction in the reactivity of the longer molecules in the system resulting in narrower MWD. This deviation is observed only for the model A because the increase in the average number of repeat units (\bar{m}_n) for models B and C in the ranges examined are small [less than 1.35 (Fig. 2)] and the reduction in the reactivities is not appreciable. This also corresponds to a smaller decrease in the diffusivities for models B and C (Figs. 3–5), and the nearly constant rate constant corresponding to linear \bar{m}_n - τ behavior. This is further seen by comparing the simulation results of weight fractions of chains of different lengths with the corresponding predictions of Flory²⁴

$$n_w(i) = \frac{iW_i}{\sum_i iW_i}, \quad (22)$$

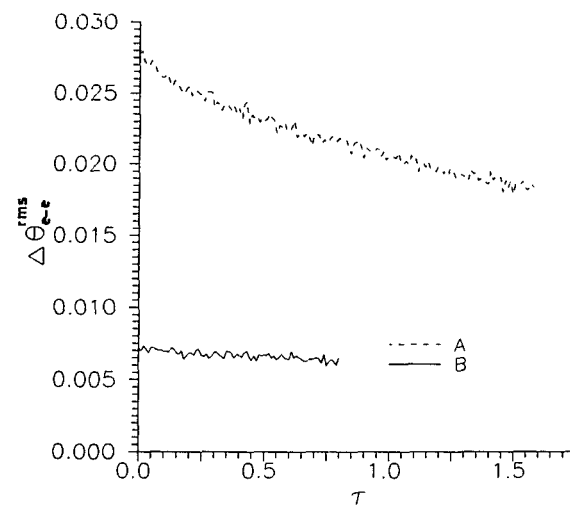


FIG. 5. Variation of the root mean square end-to-end rotation per time step of the molecules ($\Delta \theta_e^{rms}$) for the three different models with reaction time (τ) in the absence of shear flow.

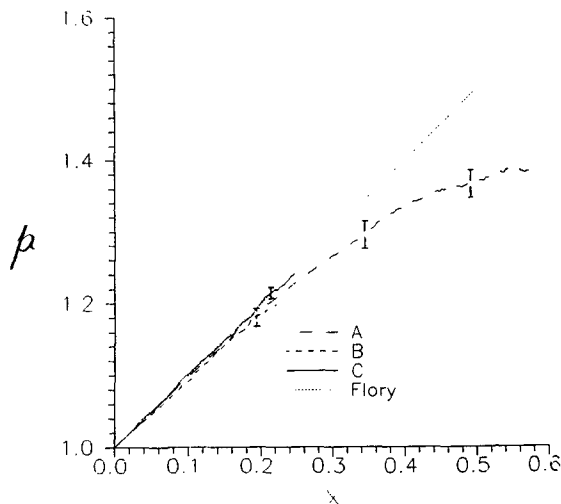


FIG. 6. Variation of the polydispersity index (p) with conversion (x) for the three different models in absence of shear flow. The result of Flory's prediction is also plotted.

where

$$W_i = x^{i-1}(1-x). \quad (23)$$

While a good match with the simulation results is seen for model A for $x < 0.25$ (Fig. 7), at higher x we note a preferential depletion and buildup of the smaller ($i=1$) and larger ($i=2$ and 3) molecules, respectively, resulting in the narrower MWD and lower polydispersity. The simulation results for models B and C, however, agree closely with the predictions of Eq. (22) for the reason mentioned above.²⁷

C. The effect of flow on reaction

In all cases, the application of shear flow increases the reaction rate (Fig. 8). This is because when the orientation

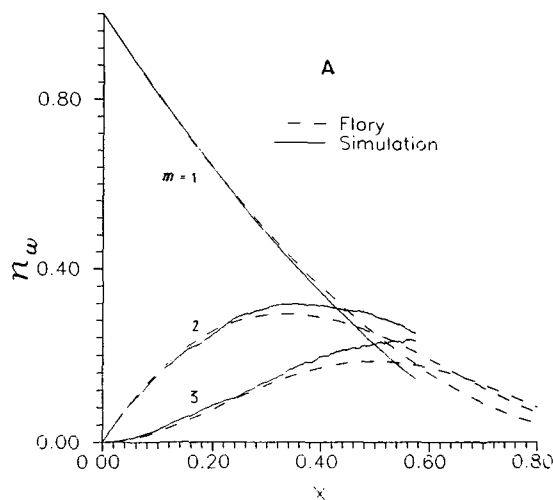


FIG. 7. Change in weight fraction [$n_w(m)$] of molecules of different size (m), with conversion (x), during reaction in the absence of flow for model A. Results of Flory's prediction are also plotted.

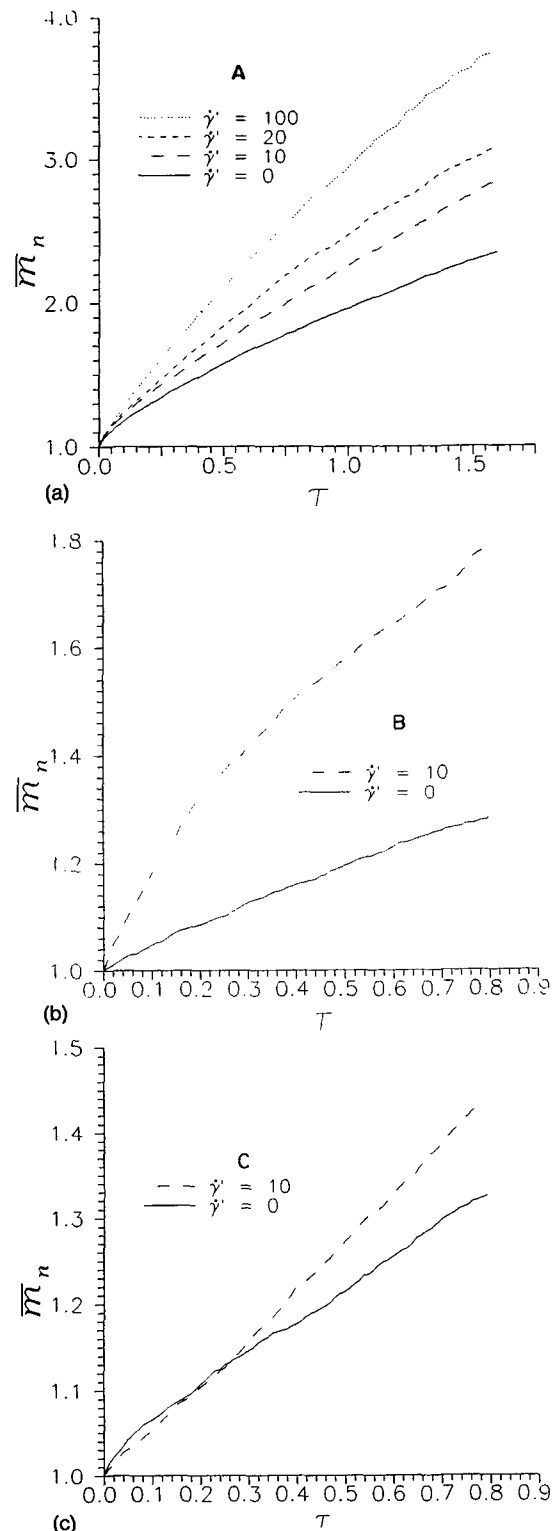


FIG. 8. Increase in the degree of polymerization (\bar{m}_n) of the molecules with time (τ), at the indicated shear rates, for models (a) A; (b) B; and (c) C.

is high, the most probable angle of approach (α_a) is in the vicinity of π , which is favored for reaction. In other words, the concentration of molecular pairs with relative orientation appropriate for reaction is higher under the shear flow, resulting in an enhanced rate of reaction. That this effect is

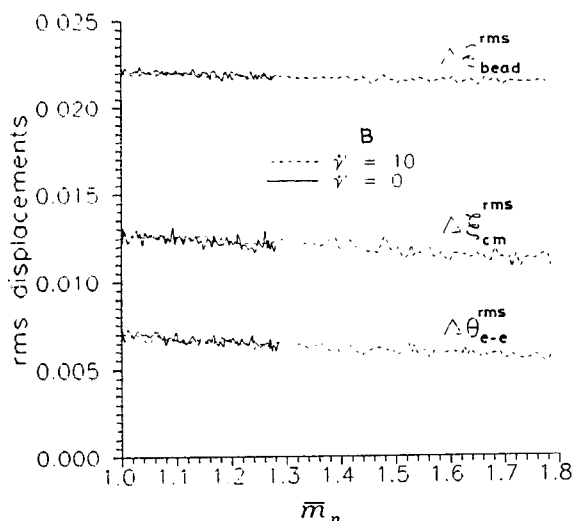


FIG. 9. Variation of the root mean square displacements and rotation per time step ($\Delta x_{\text{cm}}^{\text{rms}}$, $\Delta x_{\text{bead}}^{\text{rms}}$, $\Delta \theta_{\text{e-e}}^{\text{rms}}$) of the molecules with degree of polymerization (\bar{m}_n) with and without shear flow for model B.

not due to enhancement in the collision rate is confirmed by comparing the rms displacements for different shear rates (Fig. 9). Since the flow considered in this simulation [Eq. (4)] does not enhance the rms displacements at equilibrium (Fig. 9), when the comparison is made at same \bar{m}_n , the reaction rate enhancement under the flow corresponds to increased orientation and not the collision rate. The enhancement of reaction rate by the shear flow of $\dot{\gamma}' = 10$ is highest for the model B [Fig. 8(b)], i.e., for the longer and the more rigid chains. This is because of their higher orientation under flow caused by the smaller rotational diffusivity as evidenced by their smaller $\Delta \theta_{\text{e-e}}^{\text{rms}}$ (Fig. 5). This lower rotational diffusivity is related to the requirement of the long rigid chain that the rotation of all constituent links must be cooperative.

Figure 10 shows the variation of polydispersity index (p) with conversion (x) for model A and for $\dot{\gamma}' = 10$. The results for model A without flow are also shown in the figure. In the presence of flow, the polydispersity index is larger than the no flow case ($\dot{\gamma}' = 0$), indicating a wider MWD for the former for a fixed conversion. This is due to a larger increase in the reactivities of the longer molecules because of their higher orientation under flow. Thus the MWD for model A is wider and p is higher in the presence of flow. Similar results for cases B and C show that Flory's prediction is followed at $\dot{\gamma}' = 10$ as in absence of flow, and no effect of the flow on the MWD is seen.²⁷ This is because of the small change in length of the molecules during reaction for these cases, which results in only a slight change in reactivity of the molecules by orientation due to flow.

V. CONCLUSIONS

Brownian dynamics simulation results for diffusion controlled polymerization of three different models of bead-rod chain molecules are presented. At short time ($\tau < 0.8$), the molecular chain length is seen to increase

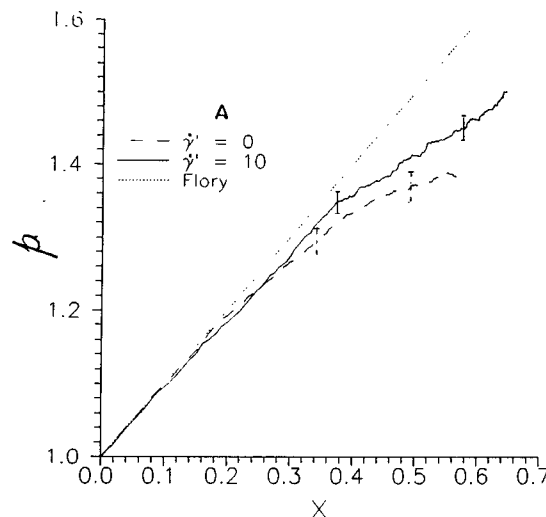


FIG. 10. Variation of the polydispersity index (p) with conversion (x) with and without flow for model A.

nearly linearly with time, and the MWD follows Flory's prediction based on the assumption of molecular reactivity being independent of chain length. The diffusivities of the longer molecules are smaller and result in their lower rates of reaction. At long times ($\tau > 0.8$), when the reduction in the molecular diffusivity with molecular length is sufficient, the rate constant for the diffusion limited reaction decreases. The MWD also deviates from the Flory prediction because of the lower diffusivity and reactivity of the longer molecules. These results are in qualitative agreement with experimental data for the polymerization of rod-like molecules which show a slowing of the reaction at high conversions and a polydispersity index lower than that predicted by the equal reactivity hypothesis.⁵

The simulations of the reaction under externally imposed shear flow show that the flow aligns the molecules along the streamlines, and increases the rate of reaction to varying degrees depending on the chain length and rigidity, and the rate of shear. The orientation increase and the influence on reaction rate is more in the case of long rigid molecules. This has implications for the production of rigid polymers. The MWD is also influenced by an applied flow, thus providing an additional parameter for control of product properties. Again the results are in qualitative agreement with experimental data for rod-like polymers.⁶

The approach presented here has the advantages of simplicity in problem formulation and the possibility of probing in detail the evolution of the polymerization reaction. Complexities such as competition effects between reactive groups, complex criteria for reaction, change in diffusivity with chain length, and imposed flow fields can easily be included as compared to theoretical analyses based on Smoluchowski's approach.¹⁰ In addition, the evolution of the product distribution is obtained in comparison to the effective rate constant obtained in the latter. The results reported in this work, however, are only qualitative because the analysis is carried out for a dilute 2D

solution with the assumption of instantaneous reaction between the end groups. Extending the analysis to 3D solutions and incorporating intermolecular interactions is relatively straightforward and would only increase the computational intensity of the problem. However, including a finite rate of reaction (which corresponds to the radiation boundary condition in Smoluchowski's approach) would require a local theoretical analysis to relate the criteria for reaction to some macroscopic system parameters.

- ¹R. T. Bailey, A. M. North, and R. A. Pethrick, *Molecular Motion in High Polymers* (Clarendon, Oxford, 1981), pp. 374–393.
- ²I. Mita and K. Horie, *J. Macro. Sci., Macro. Chem. Rev. C* **27**, 91 (1987).
- ³T. J. Tulig and M. Tirrell, *Macromolecules* **14**, 1501 (1981); **15**, 459 (1982).
- ⁴M. Tirrell and T. J. Tulig, in *Polymer Reaction Engineering: Influence Reaction Engineering Polymer Properties*, edited by K. H. Reichert and W. H. Geiseler, Proceedings of the Berlin International Workshop, 1983 (Hanser, Munich, 1984), pp. 247–268.
- ⁵D. B. Cotts and G. C. Berry, *Macromolecules* **14**, 930 (1981).
- ⁶U. S. Agarwal and D. V. Khakhar, *Nature* **360**, 53 (1992).
- ⁷A. M. North and G. A. Reed, *Trans. Faraday Soc.* **57**, 859 (1961); S. W. Benson and A. M. North, *J. Am. Chem. Soc.* **81**, 1339 (1959); **84**, 935 (1962).
- ⁸A. M. North, *Makromol. Chem.* **83**, 15 (1965).
- ⁹R. D. Bukhart, *J. Polymer Sci. A* **3**, 883 (1965).
- ¹⁰U. S. Agarwal and D. V. Khakhar, *J. Chem. Phys.* **96**, 7125 (1992).
- ¹¹U. S. Agarwal and D. V. Khakhar, *J. Chem. Phys.* **99**, 1382 (1993).
- ¹²V. G. Levich, *Physicochemical Hydrodynamics* (Prentice-Hall, Englewood Cliffs, NJ, 1962), pp. 80–87.
- ¹³P. G. De Gennes, *Radiat. Phys. Chem.* **22**, 193 (1983).
- ¹⁴A. Silberberg, in *Integration of Fundamental Polymer Science and Technology*, edited by P. J. Lemstra and L. A. Kleintjens (Elsevier, London, 1988), Vol. 2.
- ¹⁵J. L. Garcia Fernandez, A. Rey, J. J. Freire, and I. F. de Pierola, *Macromolecules*, **23**, 2057 (1990); A. Rey and J. J. Freire, *ibid.* **24**, 4673 (1991).
- ¹⁶S. A. Allison, G. Ganti, and J. A. McCammon, *Biopolymers* **24**, 1323 (1985).
- ¹⁷A. C. Balazs, C. Anderson, and M. Muthukumar, *Macromolecules* **20**, 1999 (1987).
- ¹⁸R. B. Bird, O. Hassager, R. C. Armstrong, and C. F. Curtiss, *Dynamics of Polymeric Liquids* (Wiley, New York, 1977), Vol. 2.
- ¹⁹T. A. Weber, *J. Chem. Phys.* **69**, 2347 (1978).
- ²⁰J. A. Montgomery, S. L. Holmgren, and D. Chandler, *J. Chem. Phys.* **73**, 3688 (1980).
- ²¹E. Helfand, Z. R. Wasserman, and T. A. Weber, *Macromolecules* **13**, 526 (1980).
- ²²S. Chandrasekhar, *Rev. Mod. Phys.* **15**, 1 (1943).
- ²³J. Ryckaert, G. Ciccotti, and H. J. C. Berendsen, *J. Comput. Phys.* **23**, 327 (1977).
- ²⁴P. J. Flory, in *Principles of Polymer Chemistry* (Cornell University, Ithaca, NY, 1953).
- ²⁵S. A. Rice, in *Diffusion Controlled Reactions*, edited by C. H. Bamford, C. F. H. Tipper, and R. G. Compton (Elsevier, Amsterdam, 1985).
- ²⁶D. C. Torney and H. M. McConnell, *Proc. R. Soc. London, Ser. A* **387**, 147 (1983).
- ²⁷U. S. Agarwal, Ph.D. thesis, I.I.T., Bombay, 1993.